PHYSICAL REVIEW B **78**, 041403(R) (2008)

Electronic and vibronic interactions at weakly bound organic interfaces: The case of pentacene on graphite

Pavel B. Paramonov,* Veaceslav Coropceanu, and Jean-Luc Brédas
School of Chemistry and Biochemistry, Georgia Institute of Technology, Atlanta, Georgia 30332, USA
(Received 30 May 2008; published 16 July 2008)

The electronic and vibronic processes at the interface between a pentacene monolayer and a graphite surface were characterized using a combination of density-functional theory (DFT) and dynamic vibronic coupling simulations. The electronic interactions were evaluated at the DFT level first between the highest occupied states of pentacene and the graphite surface, as well as among the pentacene molecules within a monolayer. The former are found to be ca. four times stronger than the latter for a parallel molecule/surface geometry. A dynamic vibronic model was used to analyze the interplay between the electronic and electron-vibration couplings and their effects on spectroscopic characteristics. The agreement between the simulated and experimental photoelectron spectra underlines the importance of weak electronic interactions on the vibronic coupling at the interface.

DOI: 10.1103/PhysRevB.78.041403 PACS number(s): 73.20.−r, 33.20.Wr, 68.43.−h, 71.15.Mb

Understanding of electronic processes at the interfaces between conjugated organic compounds and electrically conducting surfaces is of considerable interest in the fields of organic electronics and optoelectronics.[1,2] While chemically bound interfaces such as those formed by self-assembly of organic thiolates on the gold surface[3,4] have been studied at the atomistic level,[5–7] interfaces characterized by weak long-range attractions between molecules and a surface have not yet received the attention they deserve from the theoretical standpoint. Recently, it was shown that the interaction between an organic monolayer and a substrate can result in a strong substrate-mediated electronic coupling between the molecules within the monolayer.[8] High-resolution ultraviolet photoelectron spectroscopy (UPS) measurements of pentacene molecules physisorbed on the graphite surface reveal that the monolayer-substrate interactions can also affect the vibrational structure of the ionization spectrum.[9] In this regard, it is useful to recall that the line shape of the first ionization band can be directly related to the polaron binding energy (reorganization energy), a key ingredient in the description of charge transport (hole transfer).[10–12] The analysis of the UPS data suggests an increase of about 20% in the reorganization energy (hole–vibrational coupling) of pentacene at the interface compared with that estimated from the pentacene gas-phase UPS spectrum.[9]

In this Rapid Communication, we address the nature of the electronic and electron-vibration interactions and their impact on the UPS spectrum and reorganization energy for a weakly bound interface formed by pentacene molecules physisorbed on the graphite surface. Our first goal is to develop a methodology capable of describing electronic coupling in weakly bound systems, based on a molecular picture. In addition, we study the interplay between electronic and electron-vibration interactions as reflected in the vibrational fine structure of the first ionization. Using our methodology, we simulate the UPS spectrum for the pentacene/graphite interface and find excellent agreement with the experimental data of Yamane *et al.*[9]

One of the challenges for structural predictions of weakly bound systems lies in accounting for long-range electron correlation.[13,14] High-level correlated methods such as coupled cluster calculations provide accurate energetics and geometry for weakly bound systems[15] but at a very high computational cost. Therefore, the use of empirical potentials derived from applications of such methods to small-size systems is an efficient means of geometry predictions for the larger systems of practical interest. Importantly, we note that while less expensive density-functional theory (DFT) methods may give inaccurate geometry predictions for weakly bound complexes, they can provide a reasonable picture regarding state mixing and electronic couplings.[12]

Structural properties of interfaces formed by pentacene on various surfaces depend on the surface electronic structure,[16] molecule-surface interactions, thermodynamic conditions, and amount of pentacene on the surface.[17] Here we mimic the structure of a pentacene *monolayer* physisorbed on the graphite surface at low temperatures by using effective interatomic potentials. The graphite surface is simulated by a single graphene sheet as the topmost graphite layer is mainly responsible for the electronic effects and binding energy.[14] The total-energy components include: (i) the pentacene-graphene interactions computed using carbon-carbon potentials $U_{C\text{-}C}$ designed for aromatic clusters:[18]

$$U_{C\text{-}C} = 34(45.8\ \exp(-3.3r_{C\text{-}C}) - 1/r_{C\text{-}C}^{6}) \quad [\text{eV}], \qquad (1)$$

($r_{C\text{-}C}$ is the carbon-carbon separation in Å); (ii) the pentacene-pentacene dispersion interactions using standard parameterization;[19] and (iii) the hard-sphere repulsion of the hydrogens belonging to neighboring pentacene molecules. A constrained minimization of the total energy was performed with the pentacene molecular planes parallel to the graphite surface, as experimentally determined for pentacene on graphite at a monolayer coverage and low temperatures.[9,20] The resulting arrangement of the molecules on a graphene sheet is depicted in Fig. 1. The orientation of the pentacene molecules with respect to graphene is reminiscent of the ABAB-type stacking of graphene layers in graphite, which is typical for aromatic clusters[18] and was also found for benzene and naphthalene adsorbed on graphene.[21] The periodic

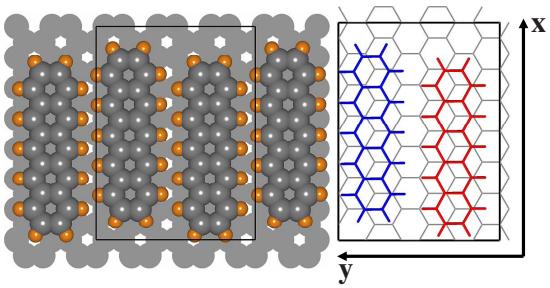

FIG. 1. (Color online) Optimized geometry of the pentacene monolayer physisorbed on a graphene sheet. Nearest-neighbor pentacene molecules are shifted with respect to each other along their long molecular axes to optimize packing and reduce repulsion among hydrogen atoms. A rectangular periodic cell is indicated. A projection on the graphene plane is shown, indicating a conformation resembling the ABAB-type stacking of graphene layers in the graphite.

cell shown in Fig. 1 contains two (symmetry) nonequivalent pentacene molecules, shifted with respect to each other along their long molecular axes. Such shifts allow closer molecular packing thus maximizing dispersion energy.

The electronic structure of the pentacene/graphene system was studied at the DFT level using the Perdew-Burke-Ernzerhof (PBE) exchange-correlation functional,[22] a plane wave basis set with 300 eV cutoff for the Kohn-Sham states of the valence electrons, and the projector augmented wave (PAW) method to describe the valence-core electron interactions,[23,24] as implemented in the Vienna *Ab initio* Simulation Package (VASP).[25] A repeated slab approach was used with a thick (~10 Å) vacuum layer above the surface to complete periodicity in the direction normal to the surface (z). We note that a trial geometry relaxation performed at the DFT level resulted in a slight increase of the pentacene-graphene separation by ca. 0.1 Å (not used in further calculations).

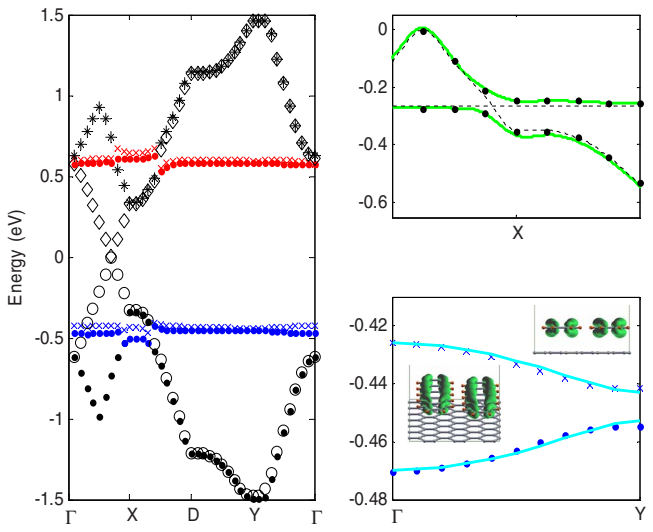

FIG. 2. (Color online) Calculated band structure for the pentacene/graphene interface in the vicinity of the Fermi level (taken as energy zero). The top-right and bottom-right panels show the band dispersion fits used to determine the pentacene-graphene and pentacene-pentacene electronic interactions. Isosurfaces of electron density for the pentacene HOMO bands at the Γ point are plotted in the insets.

Figure 2 collects the band structure along the surface (xy) plane of the pentacene/graphene system, calculated along the **k**-space path $\Gamma \rightarrow X(\frac{\pi}{a_x},0,0) \rightarrow D(\frac{\pi}{a_x},\frac{\pi}{a_y},0) \rightarrow Y(0,\frac{\pi}{a_y},0) \rightarrow \Gamma$ with the periodic cell dimensions a_x and a_y in the x and y directions, respectively. The highly dispersive bands belong to the graphene sheet; as expected, these bands intersect at the Fermi point and form a linear density of states near the Fermi level, giving graphene its semimetal character. The nearly flat states appearing at ca. −0.45 and +0.6 eV originate from the highest occupied and lowest unoccupied molecular orbitals (HOMO and LUMO), respectively, of the two symmetry nonequivalent pentacene molecules, as verified from the atom-projected partial density of states analysis. The weak dispersion of the pentacene HOMO states along the y axis (see Fig. 1) is related to direct pentacene-pentacene electronic interactions, as confirmed from the band structure obtained for the periodic system in the absence of a graphene sheet. This dispersion can be described within a one-dimensional (1D) tight-binding approximation with a (fitted) value for the *pentacene-pentacene electronic coupling* equal to 11 meV (Fig. 2, bottom right panel).

In the vicinity of the X point, the frontier states of the pentacene layer are in resonance with the graphene states; as seen from Fig. 2, the interaction between these states leads to an avoided crossing pattern. A similar result was observed for the benzene/graphite system.[26] The avoided crossing region is magnified in the top right panel of Fig. 2; there, the dispersion is plotted for a submonolayer coverage (one molecule per unit cell of Fig. 1) of pentacene on graphite to simplify the analysis (in this case, the pentacene molecules being far from each other interact only with the surface); the dashed lines represent the case when pentacene is moved far away (6 Å) from the surface (i.e., there are no interactions neither with the surface nor with nearest neighbors). The interaction between pentacene and graphene can be derived from the results of band-structure calculations using the following model:

$$\mathbf{H} = \begin{pmatrix} \varepsilon_1(\mathbf{k}) & V_{12} \\ V_{12} & \varepsilon_2(\mathbf{k}) \end{pmatrix}, \tag{2}$$

where V_{12} is the electronic coupling and $\varepsilon_1(\mathbf{k})$, $\varepsilon_2(\mathbf{k})$ are the energies of the unperturbed states of pentacene and graphene (dashed lines in Fig. 2). The avoided crossing region of the band structure is well reproduced by Hamiltonian (2) when the *pentacene-graphene electronic coupling* V_{12} is set equal to 40 meV (this value corresponds to the strongest coupling in the vicinity of the X point), as shown in Fig. 2. Thus, the pentacene-graphite electronic interactions (40 meV) are found to be about four times as large as the pentacene-pentacene interactions (11 meV).

We now turn to a discussion of the impact of these molecule-substrate interactions on the pentacene vibrational pattern and, as a result, on the line shape of the first ionization band in the UPS spectrum. Taking into account the weak interaction between pentacene and graphene, we use a simple

two-state model where the pentacene HOMO state ψ_1 is mixed with an electronic state ψ_2 that mimics the average interaction with the graphene electronic states.

Within ψ_1 and ψ_2 electronic bases, the final states contributing to the first ionization band of the system are described by the following vibronic Hamiltonian:[27]

$$\mathbf{H}_{\text{vib}} = \begin{pmatrix} H_{1,2} + l_1 Q_1 + e_1^0 & V_{12} \\ V_{12} & H_{1,2} + l_2 Q_2 + e_2^0 \end{pmatrix}, \tag{3}$$

where $H_{1,2}=T_1+T_2+\hbar(\omega_1 Q_1^2+\omega_2 Q_2^2)/2$ is the Hamiltonian of two harmonic oscillators with the dimensionless coordinates Q_1, Q_2 and frequencies ω_1, ω_2; l_1 and l_2 are the linear vibronic coupling (VC) constants, and e_1^0, e_2^0 denote the electronic energies.

The solutions of the vibronic Hamiltonian, Eq. (3), are obtained numerically by using a variational ansatz in which the vibrational part of eigenfunctions is expanded in terms of a direct-product basis of the harmonic-oscillator functions $\chi_j(Q_1)$ and $\chi_k(Q_2)$:[27,28]

$$\Phi_n(q,Q_1,Q_2) = \psi_1 \sum_{j,k} C_{jk,n}^{(1)} \chi_j(Q_1)\chi_k(Q_2) + \psi_2 \sum_{j,k} C_{jk,n}^{(2)} \chi_j(Q_1)\chi_k(Q_2), \tag{4}$$

where q denotes electronic coordinates. By limiting the total number of vibrational quanta in this expansion to a finite but large value, the solutions of this dynamic vibronic problem could be obtained with any arbitrary accuracy.

We now apply this methodology to the pentacene/graphite system and focus on the vibronic transitions that accompany photoionization in order to understand the characteristics of the experimental UPS spectrum.[9] Taking into account only the transition from the ground vibrational state to the manifold (4) of final vibronic states Φ_n with energies E_n, the spectral function $I(E)$ describing the first ionization peak is given in the framework of the Fermi golden rule by[29]

$$I(E) = \sum_n (C_{00,n}^{(1)} d_1 + C_{00,n}^{(2)} d_2)^2 \delta(E - E_n). \tag{5}$$

Here d_1 and d_2 are the electronic transition matrix elements associated with the ionization of the electronic states ψ_1 and ψ_2.[29] In the present calculations we neglect the contributions proportional to d_2. This is justified by the following: (a) the intensity of the first photoelectron transition of the pentacene is much higher than that of the graphite in the same energy region, and (b) according to our calculations, in the case of the most important lowest vibronic states, the coefficients $C_{00,n}^{(1)}$ are much larger than $C_{00,n}^{(2)}$. In the limit of $d_1 \gg d_2$, the relative intensities of transitions to vibronic states Φ_n are

$$I_n = [C_{00,n}^{(1)}]^2. \tag{6}$$

The progression given by Eq. (6) turns into the standard Poisson distribution in the case of noninteracting electronic states ($V_{12}=0$).

The extent to which a given vibrational mode is coupled to the electronic state under consideration is described by the linear vibronic constant for that mode which, in turn, is related to the Huang–Rhys factor. According to our previous

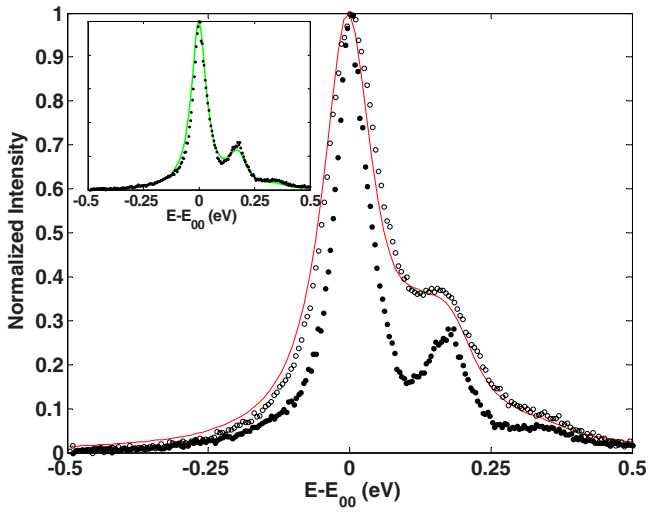

FIG. 3. (Color online) Simulated (solid line) and experimental (open circles, recorded at 49 K) (Ref 9) UPS spectra for the first ionization peak of pentacene in the pentacene/graphite system. Energy is given with respect to the 0–0 peak (E_{00}), and intensity is normalized on the peak value. A gas-phase pentacene spectrum (solid circles, 507 K) (Ref. 30) is included for comparison. The inset shows the simulated first ionization band of pentacene based on the normal-mode frequencies and Huang–Rhys factors derived from DFT calculations (Ref. 30).

DFT calculations,[30] the shape of the fist ionization band of pentacene in the gas-phase (see inset in Fig. 3) results from the interaction with several vibrational modes in the region of 1200–1600 cm^{-1}. In the present dynamic vibronic calculations, we approximated the overall effect of these modes by an effective vibrational mode with $\omega_1=1500$ cm^{-1} (186 meV) and a corresponding value of the Huang–Rhys factor $S_1=0.093$.[30] Since optical phonons in graphite have a significant density of states in the range of 1500–1600 cm^{-1},[31,32] we used the same value of 1500 cm^{-1} for both ω_1 and ω_2 for the sake of simplicity. The linear coupling constant l_2 was obtained from the best fit of the simulated spectrum to the experimental photoionization band.

Two separate cases were considered by taking as V_{12} in the Hamiltonian (3) either the pentacene-pentacene or the pentacene-graphene electronic couplings evaluated above. While the pentacene-pentacene electronic coupling within the monolayer is too small to induce noticeable changes in the vibronic progression, incorporation of the (~4 times stronger) pentacene-graphene coupling in the dynamic simulations modifies the vibronic progression significantly. When keeping the pentacene-graphene electronic coupling and the pentacene vibronic constant fixed while adjusting the value of the graphene vibronic constant (which weakly affects the vibronic progression of pentacene), we were able to achieve a very good agreement between the calculated and experimental UPS spectra presented in Fig. 3. The gas-phase spectrum of pentacene is included for comparison; it displays markedly different peak ratios in the vibronic structure. This difference highlights the importance of VC at weakly bound interfaces and the impact of electronic interactions even when comparatively small ($V_{12}/\hbar\omega=40/186<1$).

To summarize, we have developed a methodology to de-

scribe the electronic properties of a pentacene monolayer weakly bound to the graphite surface and to evaluate the *dynamic* vibronic coupling effects at the resulting interface. The parallel geometry for pentacene monolayer on the graphene sheet, preferable at low temperatures, results in the pentacene-graphene electronic coupling being much stronger than the pentacene-pentacene coupling within the monolayer. Using a vibronic coupling model along with electronic interactions evaluated at the DFT level, we have achieved quantitative agreement with the experimental photoelectron spectra. Thus, the combination of periodic DFT calculations with dynamic VC simulations provides a useful framework to understand electronic processes at weakly bound interfaces.

The authors are grateful to N. Ueno, R. Friedlein, and G. Heimel for stimulating discussions and useful suggestions. This work was supported by the Department of Energy and the National Science Foundation (under the STC Program, Contract No. DMR-0120967, and the CRIF Program, Contract No. CHE-0443564).

*Present address: Department of Physics, The University of Akron, Akron Ohio 44325, USA: pbp@uakron.edu

[1] H. Ishii, K. Sugiyama, E. Ito, and K. Seki, Adv. Mater. (Weinheim, Ger.) **11**, 605 (1999).

[2] *Conjugated Polymers and Molecular Interfaces: Science and Technology for Photonic and Optoelectronic Applications*, edited by W. Salaneck, K. Seki, A. Kahn, and J.-J. Pireaux (Dekker, New York, 2002).

[3] A. Ulman, Chem. Rev. (Washington, D.C.) **96**, 1533 (1996).

[4] J. C. Love, L. A. Estroff, J. K. Kriebel, R. G. Nuzzo, and G. M. Whitesides, Chem. Rev. (Washington, D.C.) **105**, 1103 (2005).

[5] L. Zhang, W. A. Goddard, and S. Jiang, J. Chem. Phys. **117**, 7342 (2002).

[6] G. Heimel, L. Romaner, J. L. Brédas, and E. Zojer, Phys. Rev. Lett. **96**, 196806 (2006).

[7] G. Heimel, L. Romaner, E. Zojer, and J. L. Brédas, Nano Lett. **7**, 932 (2007).

[8] R. Temirov, S. Soubatch, A. Luican, and F. Tautz, Nature (London) **444**, 350 (2006).

[9] H. Yamane, S. Nagamatsu, H. Fukagawa, S. Kera, R. Friedlein, K. K. Okudaira, and N. Ueno, Phys. Rev. B **72**, 153412 (2005).

[10] V. Coropceanu, M. Malagoli, D. A. da Silva Filho, N. E. Gruhn, T. G. Bill, and J. L. Bredas, Phys. Rev. Lett. **89**, 275503 (2002).

[11] N. E. Gruhn, D. A. da Silva Filho, T. G. Bill, M. Malagoli, V. Coropceanu, A. Kahn, and J. L. Brédas, J. Am. Chem. Soc. **124**, 7918 (2002).

[12] V. Coropceanu, J. Cornil, D. A. da Silva Filho, Y. Olivier, R. Silbey, and J. L. Brédas, Chem. Rev. (Washington, D.C.) **107**, 926 (2007).

[13] M. Dion, H. Rydberg, E. Schroder, D. C. Langreth, and B. I. Lundqvist, Phys. Rev. Lett. **92**, 246401 (2004).

[14] F. Ortmann, W. G. Schmidt, and F. Bechstedt, Phys. Rev. Lett. **95**, 186101 (2005).

[15] M. O. Sinnokrot and C. D. Sherrill, J. Phys. Chem. A **108**, 10200 (2004).

[16] G. E. Thayer, J. T. Sadowski, F. Meyer zu Heringdorf, T. Sakurai, and R. M. Tromp, Phys. Rev. Lett. **95**, 256106 (2005).

[17] A. C. Mayer, A. Kazimirov, and G. G. Malliaras, Phys. Rev. Lett. **97**, 105503 (2006).

[18] N. Lee and S. Kim, J. Chem. Phys. **122**, 031102 (2005).

[19] S. Grimme, J. Comput. Chem. **25**, 1463 (2004).

[20] H. Fukagawa, H. Yamane, T. Kataoka, S. Kera, M. Nakamura, K. Kudo, and N. Ueno, Phys. Rev. B **73**, 245310 (2006).

[21] S. D. Chakarova-Käck, E. Schroder, B. I. Lundqvist, and D. C. Langreth, Phys. Rev. Lett. **96**, 146107 (2006).

[22] J. P. Perdew, K. Burke, and M. Ernzerhof, Phys. Rev. Lett. **77**, 3865 (1996).

[23] P. E. Blöchl, Phys. Rev. B **50**, 17953 (1994).

[24] G. Kresse and D. Joubert, Phys. Rev. B **59**, 1758 (1999).

[25] G. Kresse and J. Furthmüller, Phys. Rev. B **54**, 11169 (1996).

[26] J. B. Neaton, M. S. Hybertsen, and S. G. Louie, Phys. Rev. Lett. **97**, 216405 (2006).

[27] V. Coropceanu, M. Malagoli, J. M. André, and J. L. Brédas, J. Am. Chem. Soc. **124**, 10519 (2002).

[28] S. Piepho, E. Krausz, and P. Schatz, J. Am. Chem. Soc. **100**, 2996 (1978).

[29] H. Köppel, W. Domcke, and L. Cederbaum, in *Advances in Chemical Physics*, edited by I. Prigogine and S. Rice (Wiley, New York, 1984), Vol. 57, pp. 59–246.

[30] M. Malagoli, V. Coropceanu, D. da Silva Filho, and J. L. Brédas, J. Chem. Phys. **120**, 7490 (2004).

[31] R. Nicklow, N. Wakabayashi, and H. G. Smith, Phys. Rev. B **5**, 4951 (1972).

[32] S. Piscanec, M. Lazzeri, F. Mauri, A. C. Ferrari, and J. Robertson, Phys. Rev. Lett. **93**, 185503 (2004).